Available online at www.sciencedirect.com
ScienceDirect
Journal of Molecular Catalysis A: Chemical 268 (2007) 15–23
JOURNAL OF MOLECULAR CATALYSIS A: CHEMICAL
www.elsevier.com/locate/molcata

The influence of the preparation methods and pretreatment conditions on the properties of Ag-MCM-41 catalysts

W. Gac [a,*], A. Derylo-Marczewska [b], S. Pasieczna-Patkowska [a], N. Popivnyak [b], G. Zukocinski [b]

[a] *Maria Curie-Skłodowska University, Faculty of Chemistry, Department of Chemical Technology, 3 Maria Curie-Skłodowska Sq., 20-031 Lublin, Poland*
[b] *Maria Curie-Skłodowska University, Faculty of Chemistry, Department of Adsorption, 3 Maria Curie-Skłodowska Sq., 20-031 Lublin, Poland*

Received 9 October 2006; received in revised form 29 November 2006; accepted 1 December 2006
Available online 8 December 2006

Abstract

Silver doped mesoporous silica materials MCM-41 were prepared by the direct hydrothermal (DHT) and template ion exchange (TIE) methods. The properties of materials were investigated by the adsorption/desorption of nitrogen, X-ray diffraction (XRD), and photoacoustic infrared spectroscopy (FT-IR/PAS). Redox properties were studied by the temperature programmed reduction method and temperature programmed CO oxidation test reaction. It was found that the introduction of small amounts of silver caused structural changes of the silica materials. Silver species in the catalysts obtained by the TIE method were strongly dispersed on the silica support. XRD and TPR studies of the catalysts prepared by the DHT method indicated co-existence of the large crystallites and isolated silver ions in the silica material. Studies revealed the strong influence of the pretreatment and reaction conditions on the performance of catalysts in the oxidation of CO. Reduction of catalysts was necessary to obtain high activity at low temperatures. Complex deactivation processes were recorded above 300 °C.

Keywords: Silver catalysts; MCM-41; XRD; TPR; CO oxidation

1. Introduction

Silver catalysts have found wide industrial and environmental applications, including production of formaldehyde, epoxidation of ethylene, NO_x abatement and deep hydrocarbon oxidation. The oxidative properties of silver catalysts are very sensitive to the preparation method, pretreatment or reaction conditions, composition, crystallite size, and they are not fully recognized yet [1–4]. These catalysts have been tested for many reactions, such as selective reduction of NO to N_2 [5–7], oxidation of ammonia to N_2 [8], CO_2 hydrogenation to methanol [9,10] or preferential oxidation of carbon monoxide in the product stream of methanol and gasoline reformers used to produce hydrogen fuel for fuel cells [11]. Silver has been often utilized as a modifier or main component of catalytic systems for deep oxidation reactions [12–17]. On the other hand, silver has been also used in the material and optical science, separation technology and pharmacy [18,19]. High versatility of silver catalysts is often regarded as a result of the presence of various Ag–O interactions. Oxygen can be present in the catalysts as physically or chemically adsorbed on the surface, which in general favours deep oxidation reactions; as lattice oxygen, located in the bulk-usually treated as inactive, and in the intermediate forms (e.g. oxygen intercalated in the subsurface region) which are responsible for selective oxidation reactions.

MCM-41 type mesoporous silica materials have found great interests in the recent years [20–24]. Their unique features are the extraordinarily regular structure, very narrow pore size distribution, and large surface area (often above 1000 m^2/g). The arrangement of regular parallel pores in the MCM-41 type materials resembles in some way the honeycomb structure. The properties of these materials are strongly related to the preparation methods and thermal treatment conditions. The size of pores can be easily controlled by using surfactants with different number of carbon atoms (e.g. dodecyl-, hexadecyl- or octadecyltrimethylammonium bromide) or different types of surfactants (e.g. Plurocnic-123), as well as an introduction of auxiliary compounds (e.g. 1,3,5-trimethylbenzene). The structural, adsorptive or catalytic properties can be easily modelled by the introduction of different species by various techniques,

* Corresponding author. Tel.: +48 815375526; fax: +48 815375565.
E-mail address: wojtek@hermes.umcs.lublin.pl (W. Gac).

1381-1169/$ – see front matter © 2006 Elsevier B.V. All rights reserved.
doi:10.1016/j.molcata.2006.12.002

including direct hydrothermal (DHT), template ion-exchange (TIE), grafting or impregnation. An increase of the mechanical or thermal stability, as well as the creation of new acid–base sites in the materials have been achieved by the replacement of Si cations in the framework by the Al, Ti or Ga cations. New types of hydrogenation or oxidation catalysts have been prepared by the embedding of small metal crystallites (e.g. Pt, Pd, Au or Ni), reducible oxide species (e.g. Mn, Cr, V, Mo) or immobilization of various metal containing organic ligands. Recent literature data show that silica mesoporous materials can be used as catalysts, sorbents and host structures for preparation of new metallic, oxide or carbon materials [25,26]. Metal or oxide species can be introduced to the mesoporous silica materials by several methods. One of the simplest ways is addition of metal salts to the solution containing surfactant and silica source molecules. This technique has been successfully applied for preparation of Al, Mn, V, Co or Cu containing materials. It has been shown that the structural properties and nature of metal or oxide species are strongly related to the preparation condition, including pH of the solution, temperature and the ratio of Si/Me. The mechanism of formation of such systems is still under debate. Metal cations in the aqueous solution are coordinated by the water molecules, inorganic ligands (e.g. ammonia or chlorides) or bounded with hydroxyl groups. In the solution containing surfactant molecules (for instance octadecyltrimethylammonium bromide), depending on the complex charge (I), such species can be located around organic micelles with positive charge on the nitrogen atom (S^+) as S^+I^- pairs or in $S^+X^-I^+$ arrangement with ions (X^-). The TIE technique was first used for preparation of manganese supported MCM-41 materials, and then extended to the other metal ions [27,28]. The key feature of this technique is replacement of the surfactant cations in the as-prepared silica material by the metal ions in the solution of appropriate pH. The exchange process is related to the pH of the solution, time and the type of metal ions.

The catalytic properties of silver mesoporous silica materials have not been extensively studied. Such systems were mainly examined in the field of optical and material science [29–32] or separation technology [33,34]. However, most of them have been prepared by the impregnation of the silica support with silver nitrate and then direct decomposition of the precursor at elevated temperatures. The aim of the studies was to compare the influence of the direct hydrothermal and template ion exchange preparation methods, and the preteratment conditions on the structural, surface, redox, and catalytic properties of silver doped silica mesoporous materials.

2. Experimental

2.1. Catalyst preparation

Mesoporous silica catalysts were obtained by the modified procedures described in the literature [35]. Silver was introduced to the silica support by the direct hydrothermal (DHT) and template ion-exchange (TIE) techniques.

In order to obtain the MCM-41 materials with wide pores, the surfactant containing 18 carbon atoms in the aliphatic chain and 1,3,5-trimethylbenzene (TMB) were used. In the first method 8.5 g of octadecyltrimethylammonium bromide was dissolved in 350 ml of distilled water, then 1,3,5-trimethylbenzene was introduced to a reacting mixture. Next 30 ml of ammonium hydroxide (25 wt.%) and aqueous solution of silver nitrate (0.3 g of silver nitrate dissolved in 10 ml of water) were introduced to the synthesis mixture and stirred for 0.5 h at 40 °C. Then, tetraehylortosilicate TEOS (30 ml) was slowly introduced to the mixture. After 0.5 h of stirring the obtained product was filtered, washed with distilled water, dried at 80 °C for 2 h and calcined in air at 550 °C for 6 h. Pure silica material was prepared using the same amounts of template, ammonia and silica source, as described above. In the TIE technique, the as-synthesized silica material containing surfactant molecules in the channels was filtered and washed with distilled water. Next 0.3 g of silver nitrate was dissolved in 50 ml of water and added to the product. The mixture was stirred for 1 h, and then kept at 80 °C for 20 h. The resultant material was filtered, washed, dried, and calcined at the same conditions. All the obtained samples were separated into two grain fractions (below 0.1 mm and 0.1–0.5 mm). For further studies the second fraction containing larger grains was selected. Samples were coded according to the preparation method (DHT or TIE), the type of the surfactant (containing 18 carbon atoms in the aliphatic chain) and the support applied (MCM-41).

2.2. Catalyst characterization

The catalysts composition was determined by applying the X-ray fluorescence method (ED-XRF Canberra 1510, USA).

Porous structure of the samples was investigated by the X-ray diffraction studies (XRD) performed in the modified diffractometer DRON 3 (Russia) using Cu Kα radiation. The primary mesopore diameter (w_d) was calculated from the XRD (1 0 0) interplanar spacing d using the following equation [36]:

$$w_d = cd\left(\frac{\rho V_p}{1+\rho V_p}\right)^{1/2}$$

where c is a constant equal to 1.213 for cylindrical pores [35], ρ the pore wall density assumed to be equal to that of amorphous silica −2.2 g/cm^3 and V_p is the volume of primary mesopores.

The mesoporous structure was determined by the analysis of the nitrogen adsorption/desorption isotherms obtained volumetrically at −196 °C (77 K) using ASAP 2405N apparatus (Micromeritics Corp., USA). Before measurements the samples were outgassed (∼10^{-2} Pa) at 220 °C. The adsorption data were used to evaluate the BET specific surface area, S_{BET} (from the linear BET plots) and the total pore volume, V_t (from the adsorption at the relative pressure $p/p_0 = 0.98$) [37]. The external (macropore) surface area, S_{ext}, and the primary mesopore volume, V_p, were obtained from the α_s plot method [38] using macroporous silica gel LiChrospher Si-1000 as the reference sample [37]. The mesopore structure was characterized by the distribution function of mesopore volume calculated by applying the Barrett–Joyner–Halenda (BJH) method [36].

FT-IR/PAS spectra of the samples were recorded by means of the Bio-Rad Excalibur 3000 MX spectrometer equipped with

photoacoustic detector MTEC300 (in the helium atmosphere in a detector) over the 4000–400 cm^{-1} range at the resolution of 4 cm^{-1} and maximum source aperture. The spectra were normalized by computing the ratio of a sample spectrum to the spectrum of a MTEC carbon black standard. A stainless steel cup (diameter 10 mm) was filled with powder samples (thickness <6 mm). Interferograms of 1024 scans were averaged for each spectrum.

Reducibility of the oxide species in catalysts was determined by the temperature programmed reduction method (TPR) performed in the Altamira AMI-1 system (Zeton Altamira). In order to remove any adsorbed contaminants (e.g. CO_2 or H_2O) and standardize the samples, before reduction they were heated in the mixture of 5% O_2/He at 500 °C for 0.5 h. After cooling to room temperature the reduction process was conducted in the mixture of 6.2% H_2/Ar. The rate of temperature increase was 10 °C/min. Water evolved during reduction was removed from the carrier gas in a cold trap (at LN_2–methanol mixture temperature −98 °C) placed between reactor and thermal conductivity detector (TCD). Calibration of the TCD signal was done by injecting pulses of Ar to 6.2%H_2/Ar carrier gas.

CO oxidation was chosen as probe catalytic reaction. The measurements were performed in the Altamira AMI-1 system (Zeton Altamira) coupled via heated stainless steel capillary with the quadruple mass spectrometer HAL201RC (Hiden Analytical). U-tube quartz reactor (10 mm id) with quartz wool bed was filled with small amounts of the samples ($m = 0.02$ g). Temperature was monitored by a quartz shielded *K*-type thermocouple. Samples were initially heated in the mixture of 5% O_2/He up to 500 °C, after 0.5 h were cooled down or reduced in hydrogen for 0.5 h, and then flushed with He (30 cm^3/min) at room temperature for 15 min. After switching of the feed to the mixture containing 0.5% CO, 2.5% O_2 and He (the total flow rate was 40 cm^3/min) the temperature was increased up to 500 or 800 °C, and next decreased with the rate of 10 °C/min. Such temperature programmed manner allowed to observe and analyze deactivation processes.

3. Results and discussion

3.1. Structural properties

Composition and structural properties of the studied samples are shown in Table 1. The differences in silver content indicate different nature of the processes of silver binding to silica support. Inorganic species during silica skeleton formation can be directly incorporated into the silica framework or bounded to the surface. However, the presence of silver may cause also the formation of AgBr precipitate ($K_{sp} = 7.7 \times 10^{-13}$ mol^2 dm^{-6}).

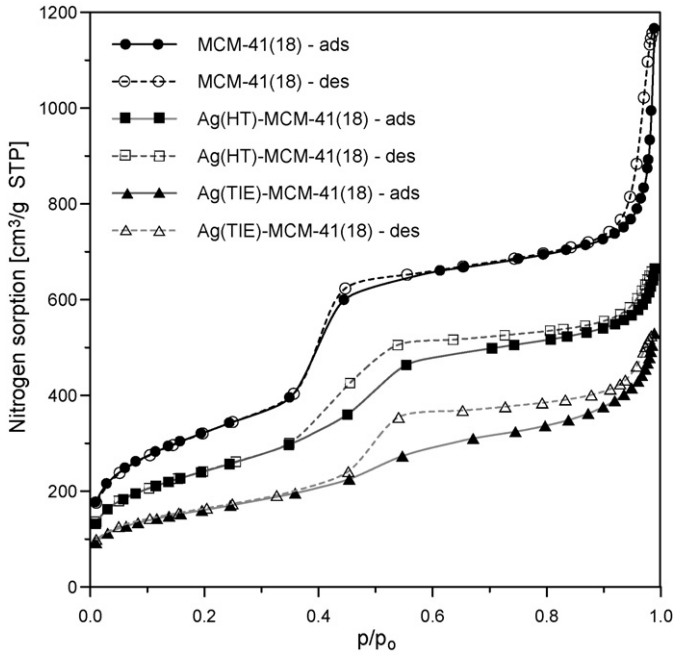

Fig. 1. The nitrogen adsorption/desorption isotherms for pure and doped with silver MCM-41 materials.

On the other hand the precipitation of AgBr can be hindered in the solution containing ammonia through formation of diamminesilver(I) complex ions $[Ag(NH_3)_2]^+$ ($K_f = 1.6 \times 10^{-7}$), which lower dissolved silver ions concentration. Silver compounds are not stable, and can be decomposed to the metallic species, especially at elevated temperatures or in the reductive environment. Thermal decomposition [39] or chemical reduction in the presence of ethanol, ethylene glycol, polyvinyl alcohol, or large surfactant molecules, e.g. Triton X-100 [31,40] has been recently utilized for preparation of silver nanoparticles. In the case of TIE technique, silica was washed before introduction of the silver precursor, hence the bromide ions were removed from the materials. The oxide species in the materials obtained by this technique are usually strongly dispersed on the silica surface. However, in the case of silver the exchange process may by perturbed by the reduction of silver ions to the metallic crystallites by the surfactant molecules or high temperature treatment.

The adsorption/desorption isotherms of nitrogen are shown in Fig. 1. The curves show distinct step over a narrow range of relative pressures $p/p_0 = 0.4$–0.55, which is typical for ordered mesoporous silica materials. The unmodified silica sample MCM-41(18) shows large surface area $S_{BET} = 1140$ m^2/g, relatively low external surface area (S_{ext}), and significant total pore volume (V_t). An introduction of silver causes structural changes. Total surface area decreases to 860 for Ag(HT)-MCM-41(18),

Table 1
Composition and structural properties of the samples

Materials	Ag (%)	S_{BET} (m^2/g)	S_{ext} (m^2/g)	V_t (cm^3/g)	V_p (cm^3/g)	*D* (nm)
MCM-41(18)	–	1150	264	1.38	0.84	3.13
Ag(HT)-MCM-41(18)	2.6	860	235	0.97	0.58	4.02
Ag(TIE)-MCM-41(18)	1.0	570	325	0.74	0.26	4.14

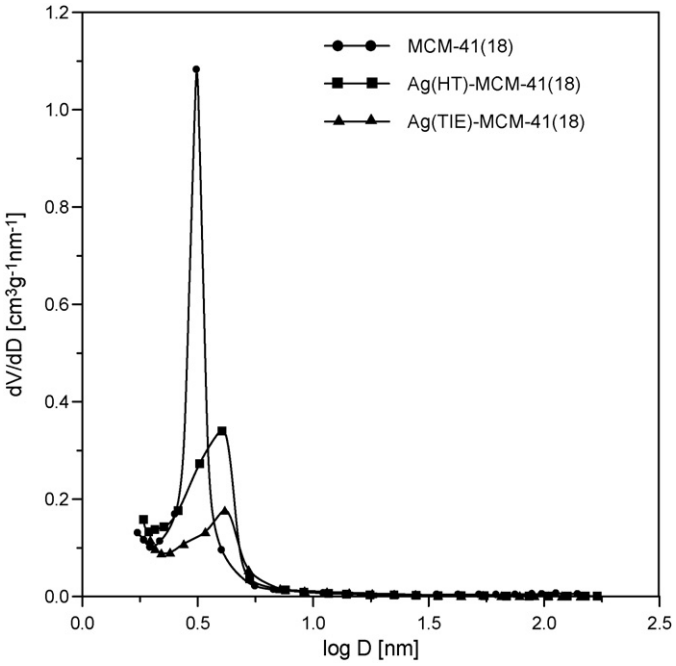

Fig. 2. Pore size distributions (PSD) of the samples.

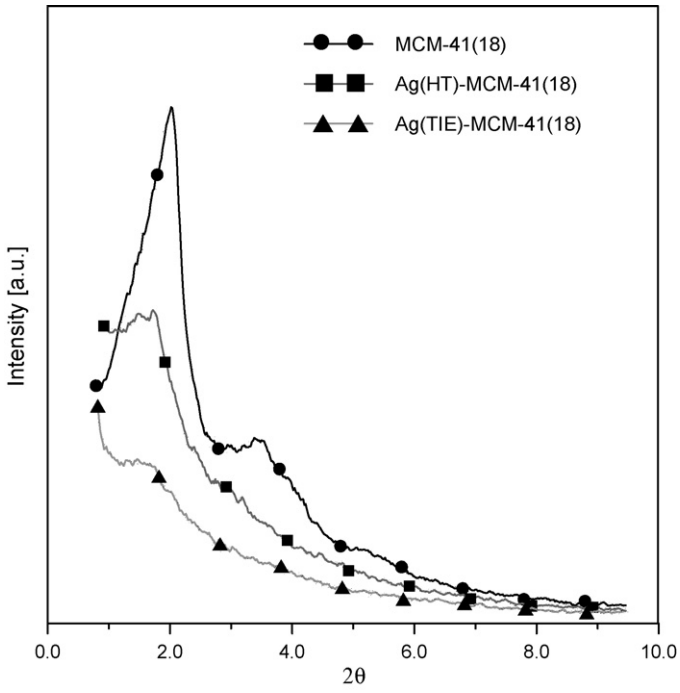

Fig. 3. XRD patterns of the samples at low diffraction angles.

and 570 m^2/g for Ag(TIE)-MCM-41(18), primary mesopore volume (V_p) decreases to 0.58 and 0.26 cm^3/g, respectively. The step on the isotherms moves to higher values of p/p_0. The courses of isotherms corresponding to the samples synthesized by using DHT and TIE methods are different over the whole pressure range. The hysteresis loop is wider for the material Ag(TIE)-MCM-41(18), which indicates that the ion-exchange method disturbs the cylindrical pores typical for MCM-41 structure and differentiate the pore sizes.

Fig. 2 shows pore size distributions, calculated according to BJH method from the adsorption branch of the isotherms. Very narrow distribution for the pure silica material indicates the uniformity of mesopores. The silver modified materials are characterized by broader distributions. It results from the introduction of heteroatom and TMB in the synthesis which disturbs the silica skeleton. In spite of larger amount of silver the Ag(HT)-MCM-41 sample shows more regular structure and higher surface area than Ag(TIE) samples. It has been shown that silver, palladium or platinum often form in the MCM-41 type materials large particles in the shape of single crystal nanowires of the size equal to pore width [9]. In the case of both synthesized samples the maximum volume occupied by silver metal is relatively low (0.95×10^{-3} and 2.5×10^{-3} cm^3/g for Ag(TIE) and Ag(HT), respectively). We can expect that only the presence of a large number of silver species distributed along the channels or blocking the entrances (e.g. at high silver loading) can influence pore volume.

The XRD patterns recorded at low diffraction angles and presented in Fig. 3 reveal regular structure of the MCM-41 silica materials. For pure MCM-41 material one observes the prominent peak and two other reflections which can be attributed to (1 0 0), (1 1 0) and (2 0 0) indices of hexagonal arrangement of pores.

The regularity of pore arrangement is worse for two Ag doped samples. The (1 0 0) peak intensity decreases in order MCM-41 > Ag(HT)-MCM-41 > Ag(TIE)-MCM-41, which confirms the structural changes observed in the nitrogen sorption studies. The calculated values of the pore size are included in Table 1.

3.2. FT-IR/PAS spectroscopy

Figs. 4 and 5 show the FT-IR/PAS spectra of the samples in the two regions. A sharp peak at 3743 cm^{-1} is connected with vibration of the isolated ≡Si–OH silanol groups. Slight shoulder with the center located at around 3650 cm^{-1} is often ascribed to the bridging hydroxyls (≡SiOH–OSi) vibrations. Stretching vibrations ν_{OH} (Si–O–H) are visible in the broad peak with the center at around 3440 cm^{-1}. Lower intensity of vibrations of the isolated silanol group in the Ag(TIE) sample may directly results from the changes of the structural properties (e.g. smaller surface area). However, such decrease may also imply that silver species are highly dispersed over silica support. Small triplet located at the shoulder of the broad band is assigned to the asymmetric CH_3, CH_2 and symmetric $CH_2 + CH_3$ vibrations. The presence of these bands unambiguously indicates the presence of the traces of template molecules. Such species are also visible in the bands at 1970 cm^{-1}, 1870 cm^{-1} as C–H vibrations, and 1630 cm^{-1} as R–NH_3^+ vibrations. Although in the studied samples the intensities of these bands are not strong, and indicate only the traces of the hydrocarbon species, the presence of these species may strongly influence catalytic activity, especially when they are located on the metal or oxide species.

The absorption bands at around 1030 and 1080 cm^{-1} are due to asymmetric stretching vibrations of Si–O–Si bridges. The absorption band at 960–970 cm^{-1} is connected with the

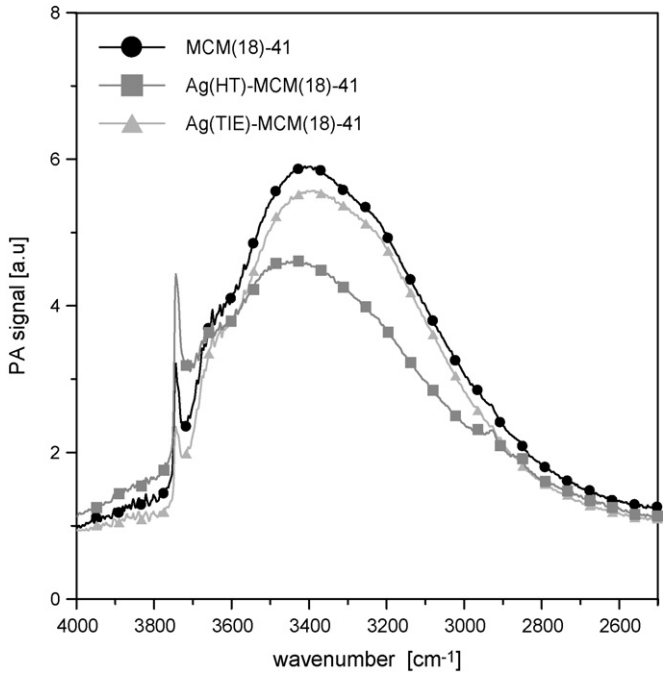

Fig. 4. FT-IR/PAS spectra of the samples at high wavenumbers.

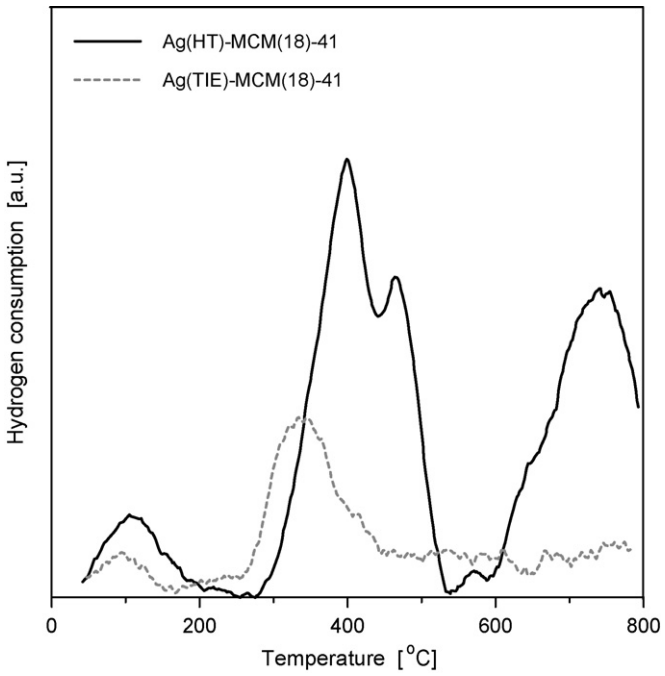

Fig. 6. TPR curves of the catalysts.

stretching vibrations of the Si–OH groups, while the bands at 780–800 cm^{-1}, and 540–560 cm^{-1} are the symmetric stretching vibrations of Si–O–Si bridges. The bands located at 450–460 cm^{-1} are assigned to the Si–O bending vibration [41,42]. Broadening of the peaks located between 1000 and 1300 cm^{-1} in the samples obtained by the TIE method indicates more amorphous nature of these materials. Similar results have been observed for the samples containing different elements prepared by the TIE method [43]. In many studies, the incorporation of metal into the silica framework has been deduced from the changes of band intensity located at 960–970 cm^{-1}, assigned to stretching vibration of the Si–O–Me linkage [44,45]. In the present studies, it has been observed a small shift of band position from 966 cm^{-1} for the MCM-41 sample to 950 cm^{-1} for the Ag(TIE)-MCM-41 sample, and the formation of the shoulder at the same position for the Ag(HT)-MCM-41 sample.

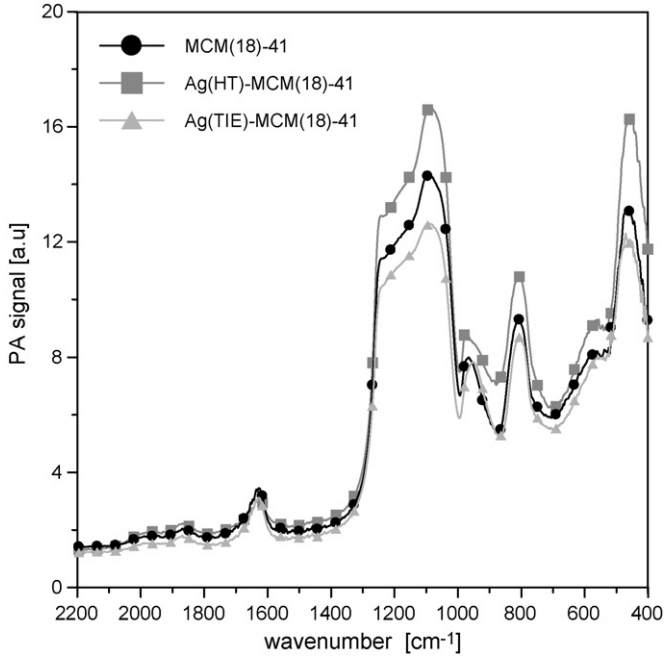

Fig. 5. FT-IR/PAS spectra of the samples at low waveumbers.

3.3. Temperature programmed reduction studies

The temperature programmed reduction curves of the samples pretreated at 500 °C, are shown in the Fig. 6. Several peaks are observed in the range of 20–800 °C. A complex shape of the TPR curves is usually associated with the reduction of oxide species on the different oxidation states and showing various interactions with support. It was often reported that position of the peaks for the supported catalysts was shifted to lower temperatures and intensity of easily reducible forms increased with increase of silver loading [46]. Silver precursors during preparation of catalysts are decomposed to the oxide forms and then partially to the metallic crystallites. In the pretreatment procedures of the TPR experiments oxygen is adsorbed at elevated temperatures on the surface of metallic silver and accommodated in the subsurface or bulk regions, forming oxide species. The TPR curves show the presence of low-temperature peak, which can be attributed to the reduction of bulk-like silver oxide phases (without strong interaction with support). Both samples show reduction peaks in the range 200–500 °C. However, the shape of the peaks for the sample obtained by the direct hydrothermal method is more complex, and shifted to higher temperatures, moreover there is also visible considerable high-temperature maximum (above 600 °C). Larger reduction peaks for Ag(HT)-MCM-41(18) sample results from higher silver loading. The

quantitative analysis revealed that consumption of hydrogen is equal to 0.132 and 0.056 mmol/g for Ag(HT) and Ag(TIE) samples, respectively. Considering silver loading this indicate the presence of the oxides with formal notation $Ag_{1.8}O$ and $Ag_{1.6}O$, respectively. The presence of different reduction peaks has been often related to the reduction of AgO or Ag_2O species of various size and location. Whereas high temperature peaks have been ascribed to the reduction of Ag^+ isolated ions [47,48]. Furusawa attributed two low-temperature peaks in the Ag-ZSM-5 catalysts to the reduction of large Ag_2O and AgO clusters located outside of the zeolite pores, while middle temperature peak—to the reduction of small Ag_2O clusters [5]. On the other hand, Shimizu showed that in the Ag-MFI catalysts all of Ag^+ was initially reduced to the $Ag_{2p}{}^{p+}$ clusters consisting of 3–4 Ag atoms, which were reduced above 400 °C to the metal particles [49]. Our studies evidenced the presence of different forms of silver oxide species in the catalysts. The samples obtained by the HT method are characterised by worse reducibility, resulting from stronger silver–oxygen bounding and stabilization of the small oxide species in the silica support.

3.4. XRD studies

The results of the XRD studies are shown in Fig. 7. Strong silver reflections are visible only on the patterns of Ag(HT) sample. The additional reflections are well suited to the AgBr phase. It is interesting that similar species have been recently reported as active components of catalysts in the visible light photocatalitic gas phase CH_3CHO oxidation [50].

The AgBr phase disappears during high temperature treatment in hydrogen atmosphere. In the samples prepared by TIE technique AgBr, oxide or metallic silver species are not visible on the XRD curves. The size of such species is below detection limit of the XRD method, and hence it is difficult to calculate their diameter. On the other hand the presence of well visible patterns for Ag(HT) sample indicates the existence of relatively large silver crystallites. Studies of the size of Ag crystallites by the XRD method in the samples after reduction in pure and diluted hydrogen did not show considerable differences (not presented here). Taking into account the TPR results it seems that Ag(HT) sample after reduction contains different types of silver crystallites—large crystallites evidenced by the XRD method and very small ones, not detected by this method but inferred from the low reducibility of the oxide phases in the TPR studies.

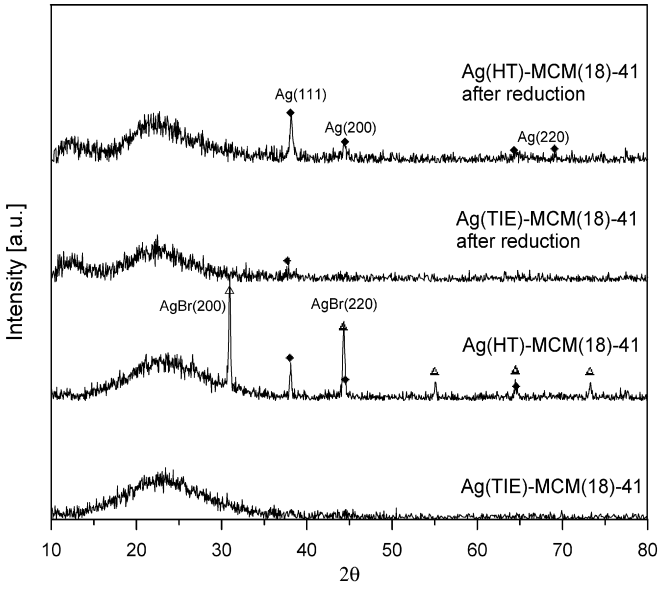

Fig. 7. XRD curves of the samples.

3.5. Oxidation of CO

Figs. 8 and 9 show the changes of CO conversion after different pretreatment conditions. Samples obtained by the DHT and TIE techniques, heated in the oxygen-containing atmosphere (5%O_2/He) up to 500 °C and then cooled down directly before reaction show very low activity. Several studies indicated that carbon monoxide can be oxidized over silver even below room temperature [51]. For Ag-MCM-41 type systems low activity (prior reduction step) can be connected with the presence of the species blocking the surface of silver crystallites, e.g. carbon from unburned template molecules, silver bromide or silica (due to strong bounding or encapsulation of silver). During the reduction process such species are removed, via silver surface reconstruction and sintering, hydrogenation and desorption of the hydrocarbon or hydrogen bromide molecules. However, the most probable reason of low initial activity is formation of the strong silver–oxygen bounding. This view can be supported by the TPR results and the changes of the performance of the reduced catalysts at high temperatures. It was shown above that after pre-treatment of the samples in the oxygen containing atmosphere silver was present in the catalysts in the form of the oxides.

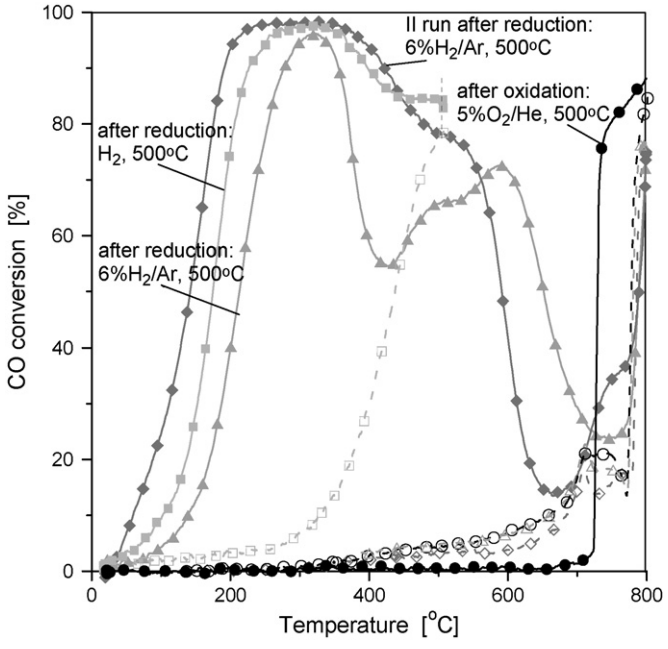

Fig. 8. CO conversion over Ag(TIE)-MCM-41 catalysts (recorded during temperature increase: filled symbols and temperature decrease: open symbols).

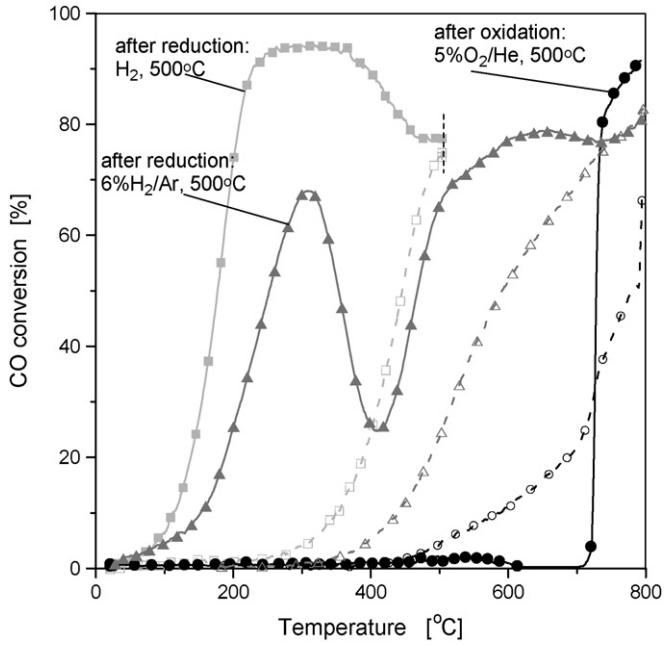

Fig. 9. CO conversion over Ag(HT)-MCM-41 catalysts (recorded during temperature increase: filled symbols, and temperature decrease: open symbols).

The activity of catalysts in the CO oxidation reaction strongly increases after reduction at 500 °C, both in pure and diluted hydrogen. The oxidation of CO is then observed almost at room temperature. Conversions monotonically increase with an increase of reaction temperature. However, at higher temperatures (250–350 °C) the oxidation process is retarded. The curves indicate some deactivation phenomena. As mentioned above the decrease of activity could be explained by the strong silver–oxygen interaction. At relatively high temperatures (700–800 °C) conversion increases again. Values recorded during temperature decrease from 800 °C (or 500 °C) are lower than that obtained during temperature increase. The hysteresis loops are formed. The extent of deactivation is related to the pre-treatment conditions. It is interesting that after reduction in pure hydrogen the activity of both samples is similar, regardless of the different silver loading and crystallite diameter (inferred from the XRD results). These results may indicate that high initial activity is related to the presence of small silver crystallites. On the other hand deactivation of the catalysts in the oxidising conditions (including CO oxidation reaction conditions) may occur more easily in the presence of such species. The activity of both types of catalysts after reduction in the diluted hydrogen is slightly worse. Lower conversions at the same temperatures are observed over the catalysts obtained by the DHT method. These catalysts above 300 °C deactivate more easily; but in the range 500–800 °C show much better activity. Another interesting observation is an increase of activity of catalysts after high temperature treatment. The initial activity of the catalysts in the second run, recorded after reaction performed up to 800 °C and then reduction at 500 °C is much better than in the first run. The catalysts show similar general deactivation trends. The results indicate that catalytic activity of the samples in the CO oxidation reaction is connected with the presence of small silver crystallites, and formation of the oxide species, which in turn are related to the preparation method, pre-treatment and reaction conditions.

The changes of activity of silver catalysts in various oxidation reactions conditions have been often discussed as a result of modification of the surface properties, related to the dispersion of crystallites or formation of strong silver–oxygen bounding. It is well-accepted opinion that deep oxidation or oxi-dehydrogenation reactions over silver surface occur with participation of the strong nucleophilic surface oxygen O_α. These species are not stable at high temperatures. Oxygen from the gas phase at such conditions may easily diffuse to the bulk of the crystallites forming subsurface O_γ or bulk O_β oxygen species, which are regarded as less active. That species take part in the selective oxidation reactions, e.g. dehydrogenation of methanol to formaldehyde. At more elevated temperatures O_β oxygen easily diffuses back to the surface, forming O_γ, O_α, which in turn can increase deep oxidation capability. Similar phenomena may occur in the confined systems of silver crystallites in the silica MCM-41 channels, and may explain the changes of activity of catalysts in the oxidation of CO. It has been reported that silver oxygen species O_α are easily formed on the defect sites or on the planes with higher surface-roughness, e.g. (1 1 0), while undisturbed (1 1 1) surfaces weakly adsorb oxygen [52]. The changes in the silver crystal morphology may strongly influence oxygen adsorption, and as a result, catalytic performance. The influence of pretreatment conditions on the surface structure has been often reported for the supported and electrolytic silver catalysts. It has been shown [53,54] that high temperature treatment in oxygen leads to the faceting of silver crystallites with predomination of (1 1 1) planes. Formation of the silver nanowires with (1 1 1) planes along the wire, parallel to the channel walls of the silica mesoporous materials SBA-15 and similar platinum particles in the MCM-41 support has been recently evidenced by Piquemal et al. [26] and Liu et al. [55]. Meima et al. [52] argued that oxygen at high temperature may adsorb and then dissolve in the silver crystallites. The removal of oxygen during reduction leads to the surface roughening. The dynamic restructuring of the electrolytic silver influenced by high temperature treatment in the methanol/oxygen atmosphere has been evidenced by Millar et al. [56] and Schlögl [1,57]. They indicated inhibition of oxygen diffusion from the bulk to the surface due to elimination of the structural defects in the temperature range of 400–600 °C, and on the other hand, the formation of new structural defects (holes) from the bulk-dissolved hydrogen and oxygen, which improved catalytic activity. Such phenomena were not reported so far to our knowledge for mesoporous silica silver catalysts and therefore need more detailed studies. For similar supported catalysts, containing gold or palladium, there were observed only some general changes of the shapes of nanoparticles confined in the mesoporous structure, attributed to the sintering along the channels [58].

4. Conclusions

We have compared structural, surface and catalytic properties of the Ag-MCM-41 materials obtained by the direct

hydrothermal synthesis and template ion-exchange methods. During preparation of the catalysts by the DHT technique the embedding of the silver species was a consequence of the detailed balance between silver–ammonia complex stability, solubility of silver bromide, decomposition of the silver compounds to the metallic crystallites, formation of Si–O–Si framework and then adsorption or incorporation of silver species into the silica mesoporous material. In the template ion exchange technique silver was added to the system containing as-prepared 'weak' silica skeleton, before the template removal. The behaviour of such systems was related to competitions of various processes, including adsorption of the cations on the outer surface of the silica support, diffusion of silver cations, replacement of surfactant molecules, and reduction of the silver ions to the metallic species inside the channels or on the outer surface of silica support. It was found that silver species obtained by the TIE technique were strongly dispersed on the silica support. The support showed less ordered structure than Ag(HT)-MCM-41 materials. XRD and TPR studies of the catalysts prepared by DHT method indicated co-existence of the large crystallites and small silver species in the silica material. AgBr species were detected in the fresh catalysts prepared by this method. Studies revealed strong influence of the pretreatment and reaction conditions on the performance of catalysts in the oxidation of CO. Reduction of catalysts was necessary to obtain high activity. Both types of catalysts showed high activity at low temperatures. Complex deactivation processes were recorded above 300 °C. Although catalysts shoved similar catalytic performance in the carbon monoxide oxidation reaction, detailed studies evidenced slightly different properties of the silver crystallites in both types of catalysts.

Acknowledgement

This work was supported by the Polish Ministry of Education and Science as research project 3T09B11429.

References

[1] A. Nagy, G. Mestl, T. Rühle, G. Weinberg, R. Schlögl, J. Catal. 179 (1998) 548–559.
[2] Ch. Karavasilis, S. Bebelis, C.G. Vayenas, J. Catal. 160 (1996) 113–205.
[3] S.V. Tsybulya, G.N. Kryukova, S.N. Goncharova, A.N. Shmakov, B.S. Bal'zhninimaev, J. Catal. 154 (1995) 194–200.
[4] C.F. Mao, M.A. Vannice, J. Catal. 154 (1995) 230–244.
[5] T. Furusawa, K. Seshan, J.A. Lercher, L. Lefferts, K.I. Aika, Appl. Catal. B37 (2002) 205–216.
[6] K.A. Bethke, H.H. Kung1, J. Catal. 172 (1997) 93–102.
[7] N. Bogdanchikova, F.C. Meunier, M. Avalos-Borja, J.P. Breen, A. Pestryakov, Appl. Catal. B36 (2002) 287–297.
[8] L. Gang, B.G. Anderson, J. van Grondelle, R.A. van Santen, Appl. Catal. B40 (2003) 101–110.
[9] S. Sugawa, K. Sayama, K. Okabe, H. Arakawa, Energy Convers. Manage. 36 (1995) 665–668.
[10] Z. Qua, M. Cheng, X. Dong, X. Bao, Catal. Today 93–95 (2004) 247–255.
[11] C. Güldür, F. Balikci, Int. J. Hydrogen Energy 27 (2002) 219–224.
[12] N. Watanabe, H. Yamashita, H. Miyadera, S. Tominaga, Appl. Catal. B8 (1996) 405–415.
[13] G.G. Xia, Y.G. Yin, W.S. Willis, J.Y. Wang, S.L. Suib, J. Catal. 185 (1999) 91–105.
[14] W. Wang, H.B. Zhang, G.D. Lin, Z.T. Xiong, Appl. Catal. B24 (2000) 219–232.
[15] S. Imamura, H. Yamada, K. Utani, Appl. Catal. A192 (2000) 221–226.
[16] L. Kundakovic, M. Flytzani-Stephanopoulos, Appl. Catal. A183 (1999) 35–51.
[17] A. Machocki, T. Ioannides, B. Stasińska, W. Gac, G. Avgouropoulos, D. Delimaris, W. Grzegorczyk, S. Pasieczna, J. Catal. 227 (2004) 282–296.
[18] H.J. Jeon, S.C. Yi, S.G. Oh, Biomaterials 24 (2003) 4921–4928.
[19] I. Sondi, B. Salopek-Sondi, J. Colloid Interface Sci. 275 (2004) 177–182.
[20] J.S. Beck, J.C. Vartuli, W.J. Roth, M.E. Leonowicz, C.T. Kresge, K.D. Schmitt, C.T.W. Chu, D.H. Olson, E.W. Sheppard, S.B. McCullen, J.B. Higgins, J.L. Schlenker, J. Am. Chem. Soc. 114 (1992) 10834–10843.
[21] X.S. Zhao, G.Q. Lu, G.J. Millar, Ind. End. Chem. Res. 35 (1996) 2075–2090.
[22] S. Biz, M.L. Occelli, Catal. Rev. Sci. Eng. 40 (1998) 207–329.
[23] D.T. On, D. Desplantier-Giscard, C. Danumah, S. Kaliaguine, Apl. Catal. A 222 (2001) 299–357.
[24] A. Taguchi, F. Schüth, Microporous Mesoporous Mater. 77 (2005) 1–45.
[25] P.V. Adhyapak, P. Karandikar, K. Vijayamohanan, A.A. Athawale, A.J. Chandwadk, Mater. Lett. 58 (2004) 1168–1171.
[26] J.Y. Piquemal, G. Viau, P. Beaunier, F. Bozon-Verduraz, F. Fiévet, Mater. Res. Bull. 38 (2003) 389–394.
[27] M. Iwamoto, Y. Tanaka, Catal. Surv. Jap. 5 (2001) 25–36.
[28] Y. Wang, Q. Zhang, Y. Ohishi, T. Shishido, K. Takehira, Catal. Lett. 72 (2001) 215–219.
[29] A. Pan, Z. Yang, H. Zheng, F. Liu, Y. Zhu, X. Su, Z. Ding, Appl. Surf. Sci. 205 (2003) 323–328.
[30] W. Cai, H. Hofmeister, T. Rainer, Physica E 11 (2001) 339–344.
[31] M.H. Lee, S.G. Oh, K.D. Suh, D.G. Kim, D. Sohn, Colloid Surf. A210 (2002) 49–60.
[32] X.G. Zhao, J.L. Shi, B. Hu, L.X. Zhang, Z.L. Hua, Mater. Lett. 58 (2004) 2152–2156.
[33] J. Padin, R.T. Yang, Chem. Eng. Sci. 55 (2000) 2607–2616.
[34] W. Cai, L. Zhang, H. Zhong, G. He, J. Mater. Res. 13 (1998) 288–295.
[35] M. Grün, K.K. Unger, A. Matsumoto, K. Tsutsumi, in: B. McEnaney, J.T. Mays, J. Rouquerol, F. Rodriguez-Reinoso, K.S.W. Sing, K.K. Unger (Eds.), Characterization of Porous Solids IV, The Royal Society of Chemistry, 1997, p. 81.
[36] M. Kruk, M. Jaroniec, A. Sayari, J. Phys. Chem. B101 (1997) 583–589.
[37] S.J. Gregg, K.S.W. Sing, Adsorption, Surface Area and Porosity, Academic Press, London, 1982.
[38] M. Jaroniec, M. Kruk, J.P. Olivier, Langmuir 15 (1999) 5410–5413.
[39] W. Chen, J. Zhang, Scr. Mater. 49 (2003) 321–325.
[40] D. Chen, L. Gao, J. Cryst. Growth 264 (2004) 216–222.
[41] R.K. Rana, R. Viswanathan, Catal. Lett. 52 (1998) 25–29.
[42] J. Ryczkowski, J. Goworek, W. Gac, S. Pasieczna, T. Borowiecki, Thermochim. Acta 434 (2005) 2–8.
[43] A. Deryło-Marczewska, W. Gac, N. Popivnyak, G. Zukocinski, S. Pasieczna, Catal. Today 114 (2006) 293–306.
[44] L.Z. Wang, J.L. Shi, J. Yu, D.S. Yan, Nanostruct. Mater. 10 (1998) 1289–1299.
[45] S. Vetrivel, A. Pandurangan, J. Mol. Catal. A217 (2004) 165–174.
[46] M. Richter, U. Bentrup, R. Eckelt, M. Schneider, M.-M. Pohl, R. Fricke, Appl. Catal. B 51 (2004) 261–274.
[47] S.W. Baek, J.R. Kim, S.K. Ihm, Catal. Today 93–95 (2004) 575–589.
[48] W.L. Dai, Y. Cao, L.P. Ren, X.L. Yang, J.H. Xu, H.X. Li, H.Y. He, K.N. Fan, J. Catal. 228 (2004) 80–91.
[49] J. Shibata, K.I. Shimizu, Y. Takada, A. Shichi, H. Yoshida, S. Satokawa, A. Satsuma, T. Hattori, J. Catal. 227 (2004) 367–374.
[50] S. Rodrigues, S. Uma, I.N. Martyanov, K.J. Klabunde, J. Catal. 233 (2005) 405–410.
[51] J.V. Barth, T. Zambelli, Surf. Sci. 513 (2002) 359–366.
[52] G.R. Meima, R.J. Vis, M.G.J. van Leur, A.J. van Dillen, J.W. Geus, F.R. van Buren, J. Chem. Soc. Faraday Trans. I 85 (1989) 279–291.
[53] G.R. Meima, R.L. Knijff, A.J. van Dillen, J.W. Geus, F.R. van Buren, J. Chem. Soc. Faraday Trans. I 85 (1989) 293–304.

[54] G.J. Millar, J.B. Metson, G.A. Bowmaker, R.P. Cooney, J. Chem. Soc. Faraday Trans. 91 (1995) 133–139.
[55] Z. Liu, Y. Sakamoto, T. Ohsuna, K. Hiraga, O. Terasaki, C.H. Ko, H.J. Shin, R. Ryoo, Angew. Chem. Int. Ed. Engl. 39 (2000) 3107–3110.
[56] G.J. Millar, M.L. Nelson, P.J.R. Uwins, J. Catal. 169 (1997) 143–156.
[57] A. Nagy, G. Mestl, D. Herein, G. Weinberg, E. Kitzelmann, R. Schlögl, J. Catal. 182 (1999) 417–429.
[58] M.T. Bore, H.N. Pham, T.L. Ward, A.K. Datye, Chem. Commun. (2004) 2620–2621.